Experimental Verification of the Individual Energy Dependencies of the Partial *L*-Shell Photoionization Cross Sections of Pd and Mo

Philipp Hönicke,[1] Michael Kolbe,[1] Matthias Müller,[1] Michael Mantler,[2,*] Markus Krämer,[3] and Burkhard Beckhoff[1]

[1]*Physikalisch-Technische Bundesanstalt (PTB), Abbestraße 2-12, 10587 Berlin, Germany*
[2]*Rigaku Corporation, 4-14-4, Sendagaya, Shibuya-Ku, Tokyo 151-0051, Japan*
[3]*AXO DRESDEN GmbH, Gasanstaltstraße 8b, 01237 Dresden, Germany*

An experimental method for the verification of the individually different energy dependencies of L_1-, L_2-, and L_3- subshell photoionization cross sections is described. The results obtained for Pd and Mo are well in line with theory regarding both energy dependency and absolute values, and confirm the theoretically calculated cross sections by Scofield from the early 1970 s and, partially, more recent data by Trzhaskovskaya, Nefedov, and Yarzhemsky. The data also demonstrate the questionability of quantitative x-ray spectroscopical results based on the widely used fixed jump ratio approximated cross sections with energy independent ratios. The experiments are carried out by employing the radiometrically calibrated instrumentation of the Physikalisch-Technische Bundesanstalt at the electron storage ring BESSY II in Berlin; the obtained fluorescent intensities are thereby calibrated at an absolute level in reference to the International System of Units. Experimentally determined fixed fluorescence line ratios for each subshell are used for a reliable deconvolution of overlapping fluorescence lines. The relevant fundamental parameters of Mo and Pd are also determined experimentally in order to calculate the subshell photoionization cross sections independently of any database.

Introduction.—The probability of the photoionization process, where a photon is absorbed and an electron is ejected from an atom, is tabulated in various data sets. These photoionization cross sections (PCSs) for exciting inner-shell electrons with x-rays depend on the photon energy as well as the electron configuration of the element of interest. Reliable knowledge of atomic fundamental parameter values such as PCSs is crucial for both conventional and modern applications in science and industry. Early works on the total PCS were based on subtracting the calculated scattering cross sections from measured mass absorption coefficients [1].

The total PCS splits up into partial cross sections for the various shells and subshells of an atom. An important question is whether the ratios between partial PCSs are constant or whether they change with energy. Both approaches exist in the calculated atomic data but a comprehensive and direct experimental answer is missing so far.

The calculations of Rakavy *et al.* [2] showed that the energetic slope of the partial PCSs strongly depends on the orbital type (*s*, *p*, or *d*) of the respective subshell and that the slopes change significantly with the orbital type. In 1973, Scofield's calculations [3] for all populated subshells of elements $Z = 1$ to 101 provided the first systematic data set based on nonrelativistic Dirac-Hartree-Slater calculations; these subshell PCS ratios are clearly energy dependent. Interpolations and fits to Scofield's data are the basis of several PCS data sets currently used [4–6]. More recent calculations by Trzhaskovskaya *et al.* [7,8] were performed

within the one-electron approximation for a free atom in the standard configuration using the central Dirac-Fock-Slater potential and by taking into account all multipoles of the radiation field. Their data is in good agreement with Scofield's PCSs (see Fig. 1).

On the other hand, there are also data sets widely used in analytical applications, such as x-ray fluorescence spectrometry (XRF), where partial PCSs are derived from the total PCS by applying constant (energy independent) jump ratios [9,10]. Major x-ray equipment manufacturers widely use jump ratio values in their quantification algorithms and also the International Union of Pure and Applied Chemistry proposes the use of constant ratios in a standard reference guide [11,12]. The ratios are defined by the jump height of the mass absorption coefficient at the respective absorption edge and are independent of the photon energy. The ratios are then used to subdivide the total PCS into the contributions of the various subshells (fixed jump ratio approximation). As Ebel [4] indicated by comparing available data sets, this produces consistent results for the *K*-shell PCS and is rather questionable for the *L* and *M* subshells. Close to the *L* absorption edges both approaches deliver similar results (by definition), but they differ significantly with increasing photon energy. As the PCSs have a direct impact on measurands such as the amount of substance, both the correct approach and values of PCS data need to be experimentally confirmed.

Kunz *et al.* [13] and Gorgoi *et al.* [14] derived PCS data for higher shells of Au and Ni respectively from x-ray
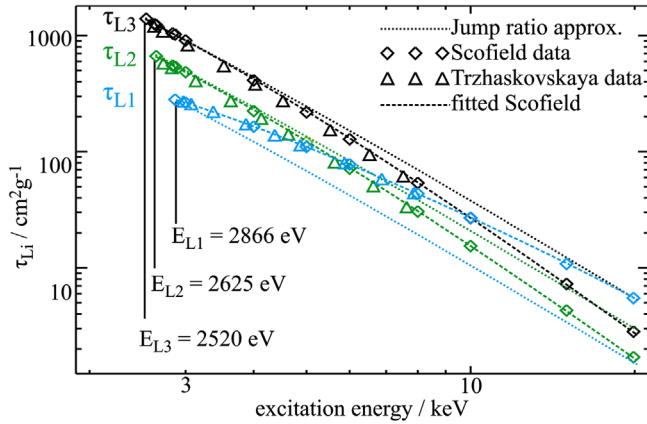
FIG. 1 (color online). Comparison of subshell PCSs (τ_{Li}) for molybdenum from different sources. The dotted lines correspond to total PCSs multiplied with energy independent jump ratios (Elam *et al.* [9]), the diamonds correspond to Scofield's calculations [3], and the triangles show the calculations by Trzhaskovskaya *et al.* [7,8]. The dashed lines are fits to Scofield's data.

photoelectron spectroscopy data. Although the experimental data of both papers show comparable energetic slopes for these subshells, their absolute values differ by up to a factor of 3 from Scofield's. Because of the diverse assumptions in data evaluation and missing uncertainties, these results do not allow for a full assessment of the reliability of Scofield's and Trzhaskovskaya's data.

Figure 1 shows a comparison of the energy independent jump ratio approach (using PCS data and jump ratios by Elam [9]) and the theoretical energy dependent subshell ratios by Scofield [3] and Trzhaskovskaya [7,8] for the molybdenum L-subshell PCSs. The differences increase with photon energy and reach a factor of about 2 for the L_2 and L_3 PCS and a factor of more than 3 for the L_1 PCS near the Mo K absorption edge. The Scofield data were interpolated using fifth order polynomials [4].

The results presented in this Letter are based on photon-in–photon-out experiments. The subshell PCSs for the three L absorption edges of Mo and Pd were determined by measuring the emitted fluorescence intensities related to each subshell as a function of the incident photon energy. By employing the radiometrically calibrated instrumentation of the Physikalisch-Technische Bundesanstalt (PTB) [15,16] and the fundamental parameter-based XRF quantification approach [15], the PCS can be derived from the fluorescence intensities. The relevant atomic fundamental parameters, e.g., the L-subshell fluorescence yields and the Coster-Kronig transition probabilities, have been determined previously [17] in order to be independent of any tabulated values.

Experimental.—For the experiments, thin layers of Mo and Pd with a nominal thickness of 250 nm on 500 nm thick silicon nitride membranes were used. The metal layers were deposited onto the membranes using magnetron sputtering

with a lateral homogeneity of the mass deposition over the entire area better than 1%.

The XRF measurements were carried out at PTB's four-crystal monochromator beam line [18] for bending magnet radiation as well as the 7-T wavelength shifter beam line [19] at the synchrotron radiation facility BESSY II. The incident photon energy was varied from below the L_3 edge up to energies just below the K edge.

An ultrahigh-vacuum chamber and a silicon drift detector calibrated with respect to its detector response functions and detection efficiency [20], as well as calibrated photodiodes [15] were used to monitor the incident photon flux. Both the incident beam and the detector formed an angle of 45° with respect to the sample surface.

Absorption correction factors were determined by transmission measurements using the same samples as for the XRF measurements in the identical geometry and for the same incident x-ray beam energies as well as for photon energies of the fluorescence emission lines. Thus, the knowledge of the absorption is independent of any database values for mass attenuation coefficients.

The recorded XRF spectra were evaluated using fixed fluorescence line ratios for each subshell lineset convolved with the known detector response functions. The transition probabilities, defining these fixed linesets, were derived from the spectra by successively tuning the incident energy across the L edges (see Ref. [17] for details). For spectra excited with photons far above the L_1 edge, fixed linesets for all subshells were used to deduce the fluorescence intensities. An example for molybdenum excited at 2.95 keV is shown in Fig. 2.

By employing fixed linesets rather than single fluorescence lines, the numerical stability of the fitting was significantly increased and the uncertainties for the
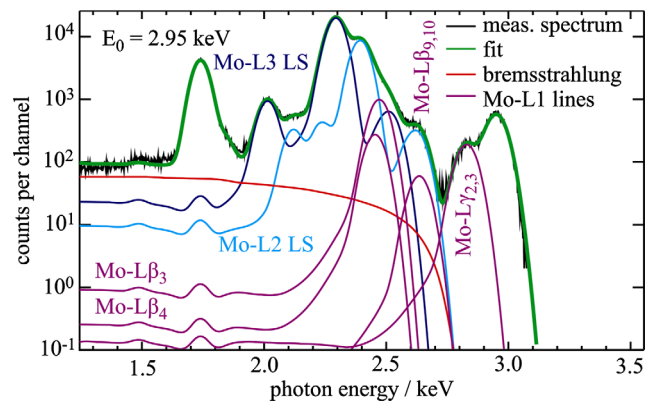
FIG. 2 (color online). Spectrum of Mo recorded at an incident photon energy of 2.95 keV and its fit employing fixed linesets (LS) of fluorescence lines for the L_3 and the L_2 subshells, the single fluorescence lines of the L_1 subshell and a bremsstrahlung background originating from Mo-M photoelectrons. Si-K fluorescence radiation emitted from the membrane at 1.74 keV and scattered incident radiation at 2.95 keV are visible as well.

determination of the fluorescence intensities could be reduced to 1.5% [17]. The PCSs of the respective subshell at an incident energy of E_0 were calculated following Sherman's equation [21] using the determined values for the L-subshell fluorescence yields as well as the Coster-Kronig transition probabilities [17].

By deriving all relevant parameters for the calculation of the PCS from either the calibrated equipment or the measurements, the obtained PCS data are independent of any tabulated fundamental parameter values. The absolute areal mass of the metal layer was determined from transmission measurements by fitting the measured mass absorption coefficients in the energy range between 4 and 7 keV to Ebel's data [4]. This has been validated by using the experimental mass absorption coefficients of Ménesguen for Mo [22], measured on thin foil samples with independently determined areal mass [23]. Assuming a relative uncertainty of 5% [24] for the tabulated data, the results are well in line with each other. The uncertainty of the areal mass does not influence the overall energetic behavior of the subshell PCSs.

The PCSs for the Mo-L and the Pd-L absorption edges have been experimentally determined with relative uncertainties in the range from 5% to 30%. Because of the Coster-Kronig coupling between the L edges and the energy dependent ratios between the L_1 PCS and the L_3 and L_2 PCS, the uncertainties for L_3 and L_2 depend on the photon energy (see Figs. 4 and 5). Close to the respective absorption edge the uncertainty is lower compared to the region just below the K edge. Main contributions to the uncertainty budget are the uncertainties of the determined Coster-Kronig factors (see Ref. [17]), the solid angle of detection, and the areal mass of the respective metal layer.

Results and discussion.—The experimental results for the Mo PCS are shown on the left-hand side of Fig. 3. The data was modeled with fifth order polynomial functions similar to Ref. [4] using weighted least-squares

fits (solid lines). The qualitative behavior of the experimental data is very similar to the calculations of Scofield and Trzhaskovskaya: both the nearly parallel curves of the L_3 and L_2 PCSs as well as the significantly nonparallel L_1 PCS match the experimental data well.

The right side of Fig. 3 shows comparisons between the fitted experimental results and the likewise interpolated Scofield and Trzhaskovskaya data; they differ by up to 20% with respect to the absolute values of the L_1, L_2, and L_3 data but exhibit a rather congruent energetic behavior. For comparison with our experimentally determined data, the ratio between our data and the two calculations is depicted. Close to the respective absorption edges the agreement of the absolute values with the Scofield L_2 and L_3 data as well as with Trzhaskovskaya's L_3 data is within 5% and remains within our uncertainty interval up to 20 keV. Trzhaskovskaya's data for both the L_2 and the L_1 PCS are reproduced less well by the experimental data, showing significantly larger deviations. Regarding the energetic behavior, the agreement between our data and both sets of calculated data is very similar for all three subshell PCSs and provides a clear experimental evidence for the energy dependence of PCS ratios being in contrast to the constant jump ratio concept. The ratios to Scofield data decrease for L_2 and L_1, and increase for L_3 with increasing photon energy. These deviations are partly caused by the uncertainty of the Coster-Kronig coefficients, the influence of which increases with the photon energy as already mentioned. The relative uncertainties of the L_3 and L_2 PCS show a similar increasing behavior with photon energy, while the uncertainty for the L_1 PCS is constant over energy since no Coster-Kronig events need to be accounted for. This is depicted in the inset of Fig. 3.

The left side of Fig. 4 shows the experimental results for palladium together with the fits. Again, the general behavior of the subshell PCSs agrees well with the theoretical calculations regarding their energy dependence. In contrast
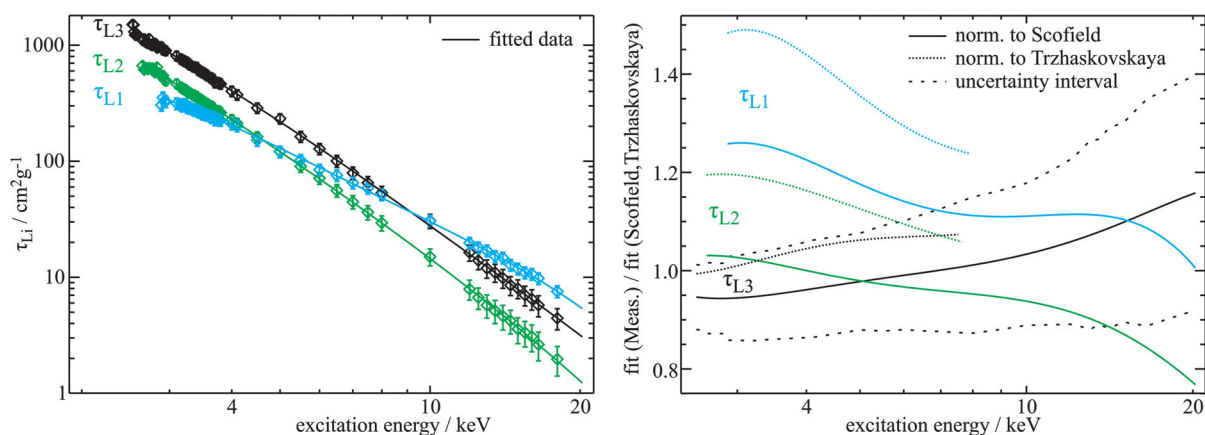
FIG. 3 (color online).   Experimentally determined PCSs for the Mo-L subshells and fifth order polynomial fits (solid lines) as well as the relative uncertainties in the inset. The right figure shows comparisons to Scofield's data [3] (solid lines) and Trzhaskovskaya's data [7,8] (dotted lines).
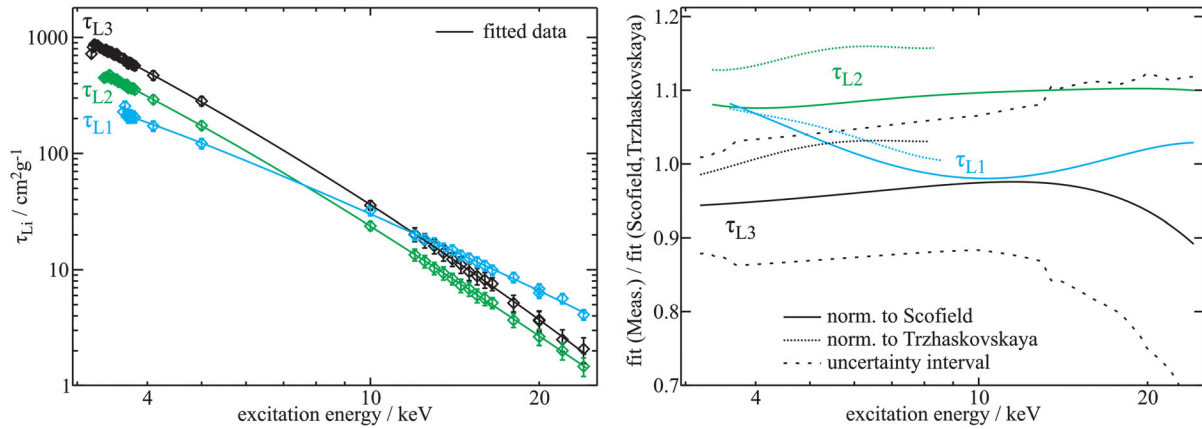
FIG. 4 (color online).   Experimentally determined PCSs for the *L* subshells of Pd and fifth order polynomial fits (solid lines) as well as the relative uncertainties in the inset. Comparisons to Scofield data [3] (solid lines) and Trzhaskovskaya data [7,8] (dotted lines) are shown on the right-hand side.

to the results for molybdenum, the agreement between the subshell PCSs with both the Scofield and the Trzhaskovskaya data is very good, yielding less than 10% difference for the absolute values over the whole energy range. Only Trzhaskovskaya's L_2 PCS show a higher difference with respect to their absolute value. The energetic behavior of the experimental Pd L_3 PCS shows good agreement with Scofield's up to 10 keV and even better agreement with Trzhaskovskaya's L_3 PCS. The Pd L_2 PCS show only minor variations over energy compared to Scofield's whereas the Pd L_1 PCS deviates at both low and high photon energies. The deviations close to the Pd K edge are caused by the increasing influence of the Coster-Kronig coefficients and the resulting relative uncertainties of the Pd L_3 and L_2 data just below the K absorption edge (see the inset of Fig. 4). Because of the

missing experimental results between 5 and 10 keV, the observed deviations for the L_1 PCS with respect to Scofield's data in this energy range could be an artifact of the fitting.

Figure 5 shows a comparison between some of the widely used data sets for subshell PCSs. The experimental results for the Pd L_1 PCS were used to evaluate the different approaches in the literature, since the deviations between Scofield's calculations and the jump ratio approximation are especially significant for the L_1 PCS. The subshell data based on Scofield's calculations [3], which are the basis of the compilations of Ebel [4] and Cullen [6], as well as the X-raylib database [5], are confirmed by our experimental data. All three compilations provide nearly identical values for Pd L_1. The Elam [9] and McMaster [10] data, where the total PCSs are split up into the subshell data by applying the jump ratio approximation, deviate significantly from the experimentally determined results by up to 300%.

The energetic dependence of the *L* subshell PCSs as predicted by Scofield [3] and Trzhaskovskaya *et al.* [7,8] was experimentally validated exemplarily for Mo and Pd by a reliable photon-in–photon-out experiment. The PCSs have been determined for incident photon energies ranging from the respective L_3 absorption edges up to the K absorption edges. For higher photon energies, additional effects, e.g., cascade effects [25] or interchannel coupling [26], would have to be considered. Other fundamental parameters relevant for the calculation of the cross sections from the measured fluorescence intensities were determined experimentally as well [17]. Both the energetic behavior of the L_3, L_2, and L_1 cross sections and the absolute values show a rather good agreement with the data of Scofield [3] and Trzhaskovskaya *et al.* [7,8]. The absolute values of Scofield's calculations are more in line with the experiments, showing maximum deviations of 25% for Mo and remain within 10% for the Pd data. For
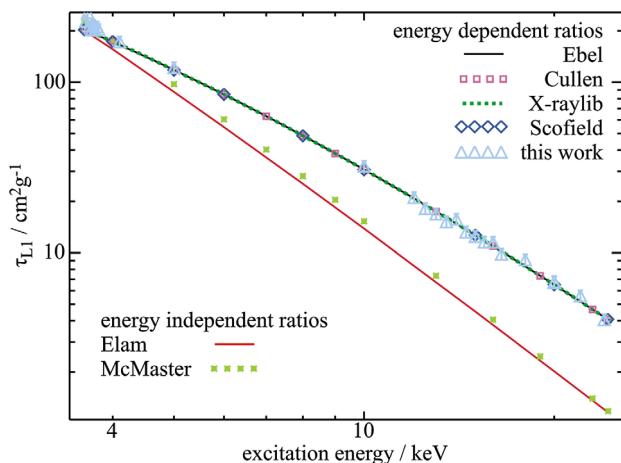
FIG. 5 (color online).   Experimentally determined PCSs for the Pd-L_1 absorption edge in comparison to the data of Ebel [4], Cullen [6], X-raylib [5], and Scofield [3], as well as McMaster [10] and Elam data [9]. The McMaster and Elam data were calculated from the total PCS using the jump ratio approximation.

both elements the overall agreement of the experimental data with calculated L_3 PCS is better than for the L_2 and L_1 PCSs. Scofield's data for L_2 and L_1 deviate less from the experimental data for both elements. For Pd Trzhaskovskaya's L_3 PCS is in better agreement with the experiment than Scofield's L_3 data, while the experimental L_2 and L_1 PCS are more in line with Scofield's calculations. However, the determined energy dependencies of the subshell PCS are less reliable in the vicinity of the K absorption edges due to the increased experimental uncertainties.

More accurate knowledge of subshell PCSs is crucial for the quantification reliability of many x-ray analytical methods such as x-ray photoelectron spectroscopy [27] and x-ray fluorescence analysis [15]. In particular, when characterizing nanomaterials, no or only few reference materials are available for calibration purposes. Here, the knowledge of atomic fundamental parameters such as PCSs is indispensable for compensating for missing reference materials.

———————————

[*]Permanent address: Fl.Trautenberger Straße 26, 3002 Purkersdorf, Austria.

[1] J. H. Hubbell, Phys. Med. Biol. **51**, R245 (2006).

[2] G. Rakavy and A. Ron, Phys. Rev. **159**, 50 (1967).

[3] J. H. Scofield, Lawrence Livermore National Laboratory, Report No. UCRL-51326, 1973.

[4] H. Ebel, R. Svagera, M. F. Ebel, A. Shaltout, and J. H. Hubbell, X-Ray Spectrum. **32**, 442 (2003).

[5] T. Schoonjans, A. Brunetti, B. Golosio, M. Sanchez del Rio, V. A. Solé, C. Ferrero, and L. Vincze, Spectrochim. Acta B Atom. Spectros. **66**, 776 (2011).

[6] D. E. Cullen, J. H. Hubbell, and L. Kissel, Lawrence Livermore National Laboratory, Report No. UCRL-50400, Vol. **6**, Rev. 5, 1997.

[7] M. B. Trzhaskovskaya, V. I. Nefedov, and V. G. Yarzhemsky, At. Data Nucl. Data Tables **77**, 97 (2001).

[8] M. B. Trzhaskovskaya, V. I. Nefedov, and V. G. Yarzhemsky, At. Data Nucl. Data Tables **82**, 257 (2002).

[9] W. T. Elam, B. D. Ravel, and J. R. Sieber, Radiat. Phys. Chem. **63**, 121 (2002).

[10] W. H. McMaster, N. K. Del Grande, J. H. Mallett, and J. H. Hubbell, At. Data Nucl. Data Tables **8**, 443 (1970).

[11] M. Mantler, J. P. Willis, G. R. Lachance, B. A. R. Vrebos, K.-E. Mauser, N. Kawahara, R. M. Rousseau, and P. N. Brouwer, in *Handbook of Practical X-Ray Fluorescence Analysis*, edited by B. Beckhoff, B. Kanngießer, N. Langhoff, R. Wedell, and H. Wolff (Springer-Verlag, Berlin Heidelberg, 2006), pp. 309–410.

[12] J. Inczedy, T. Lengyel, and A. M. Ure, *International Union of Pure and Applied Chemistry (IUPAC) Compendium of Analytical Nomenclature:Definitive Rules*, 3rd ed. (Blackwell Science, Oxford, UK, 1998).

[13] C. Kunz, S. Thiess, B. Cowie, T.-L. Lee, and J. Zegenhagen, Nucl. Instrum. Methods Phys. Res., Sect. A **547**, 73 (2005).

[14] M. Gorgoi, F. Schäfers, S. Svensson, and N. Mårtensson, J. Electron Spectrosc. Relat. Phenom. **190**, 153 (2013).

[15] B. Beckhoff, J. Anal. At. Spectrom. **23**, 845 (2008).

[16] J. Lubeck, B. Beckhoff, R. Fliegauf, I. Holfelder, P. Hönicke, M. Müller, B. Pollakowski, F. Reinhardt, and J. Weser, Rev. Sci. Instrum. **84**, 045106 (2013).

[17] M. Kolbe, P. Hönicke, M. Müller, and B. Beckhoff, Phys. Rev. A **86**, 042512 (2012).

[18] M. Krumrey and G. Ulm, Nucl. Instrum. Methods Phys. Res., Sect. A **467**–**468**, 1175 (2001).

[19] W. Görner, M. P. Hentschel, B. R. Müller, H. Riesemeier, M. Krumrey, G. Ulm, W. Diete, U. Klein, and R. Frahm, Nucl. Instrum. Methods Phys. Res., Sect. A **467**–**468**, 703 (2001).

[20] F. Scholze and M. Procop, X-Ray Spectrum. **30**, 69 (2001).

[21] J. Sherman, Spectrochim. Acta **7**, 283 (1955).

[22] Y. Ménesguen and M.-C. Lépy (private communication).

[23] J. M. Sampaio, T. I. Madeira, J. P. Marques, F. Parente, A. M. Costa, P. Indelicato, J. P. Santos, M.-C. Lépy, and Y. Ménesguen, Phys. Rev. A **89**, 012512 (2014).

[24] P. Caussin, Powder Diffr. **28**, 90 (2013).

[25] D. Sokaras, A. G. Kochur, M. Müller, M. Kolbe, B. Beckhoff, M. Mantler, Ch. Zarkadas, M. Andrianis, A. Lagoyannis, and A. G. Karydas, Phys. Rev. A **83**, 052511 (2011).

[26] W. Drube, T. M. Grehk, S. Thieß, G. B. Pradhan, H. R. Varma, P. C. Deshmukh, and S. T. Manson, J. Phys. B **46**, 245006 (2013).

[27] A. Jablonski, B. Lesiak, L. Zommer, M. F. Ebel, H. Ebel, Y. Fukuda, Y. Suzuki, and S. Tougaard, Surf. Interface Anal. **21**, 724 (1994).